Available online at http://scik.org
Commun. Math. Biol. Neurosci. 2020, 2020:16
https://doi.org/10.28919/cmbn/4506
ISSN: 2052-2541

MODELLING THE EBOLA VIRUS DISEASE DYNAMICS IN THE PRESENCE OF INTERFERED INTERVENTIONS

MAUREEN L. JUGA*, FARAI NYABADZA

Department of Mathematics and Applied Mathematics,

University of Johannesburg, Johannesburg, South Africa

Abstract. The recent Ebola virus disease (EVD) has been difficult to eradicate in the Democratic Republic of Congo (DRC) due to the presence of war and political instability which stand in the way of disease control, such as; hospitalization, vaccination, construction and successful running of EVD treatment units and proper functioning of intervention teams in some parts of the country. Interrupted control usually leads to an increase in disease transmission, hence making eradication very difficult or even impossible. In this paper, we develop a deterministic model for EVD dynamics in the presence of war. the model's steady states are determined. The model has an Ebola free equilibrium and a unique endemic equilibrium whose existence is subject to the epidemic threshold $R(\omega)$ that is a function interference parameter. The global stabilities of the equilibria are determined. We fit this model to observed data and evaluate the impact of war on EVD evolution and make suggestions that may influence policy direction in the management of EVD epidemic. Our results quantify the negative effects of war on EVD control, thus presenting the usefulness of mathematical models in disease management.

Keywords: Ebola virus disease; level of war; hospitalization; epidemic; model fitting.

2010 AMS Subject Classification: 92B05.

*Corresponding author

E-mail address: maureenlenna@yahoo.com

Received February 7, 2020

1. INTRODUCTION

Ebola virus disease (EVD) [6], is one of the most dangerous filoviruses that causes a viral hemorrhagic fever in humans. The first outbreak of the disease started in 1976 in the Democratic Republic of Congo (DRC) [2]. The name Ebola is the name of a river in the North west of the DRC where the first EVD cases were noticed. There are five stains of the virus,namely, the Sudan Ebola virus species, Bundigbuyo Ebola virus species, Taï forest Ebola virus species and Reston Ebola virus species. The Zaire Ebola virus species is the most dangerous species and has a case fatality rate of 60-90%, [2, 6].

Ebola virus is transmitted to humans by animals. Rodents and bats have always been considered as potential Ebola virus reservoirs [6]. Ebola is a fluid borne disease and Human infections occur after unprotected contact with infected patients. After contamination, symptoms can appear from 2 to 21 days later and the infectious period can last from 4 to 10 days [18]. Once an individual is infected, the virus rapidly replicates and attacks the individual's immune system. So, depending on the individual's immune system, the individual can immediately die or recover after treatment. According to the World Health Organisation (WHO), an infected individual usually have at least three of the following symptoms: headaches, anorexia, lethargy, aching muscles or joints, breathing difficulties, vomiting, diarrhoea, stomach pain, inexplicable bleeding, or any sudden inexplicable death [8].

Laboratory diagnostic of the Ebola virus is done through the measurement of the host-specific immune response to infection and the detection of virus particles. Reverse Transcription Polymerase Chain Reaction and antigen detection (ELISA) are the primary assays to diagnose an acute infection [6].

There is no confirmed treatment against Ebola disease although recently, there have been reports on the discovery of a new Ebola cure in the Democratic Republic of Congo (DRC). The New York Times Magazine, on the 12th August 2019 reported the discovery of two antibody-based treatments namely, REGN-EB3 and mAb-114 which saved roughly 90% of the patients who were newly infected. It continued that, the two experimental treatments are working so well that they will now be offered to all patients in the Democratic Republic of Congo. Also, the

antibody-based treatments are quite powerful and they raise hopes that the disastrous epidemic in eastern Congo can soon be stopped and future outbreaks more easily contained. The treatments (REGN-EB3 and mAb-114), are both cocktails of monoclonal antibodies that are infused intravenously into the blood [28]. The Healthline magazine also reported that two people with Ebola who were treated with the treatment in the city of Goma in the Democratic Republic of the Congo (DRC) have been declared cured [29].

Mathematical modelling provides a unique approach to gain insightful knowledge of EVD transmission and control dynamics. Based on this knowledge, effective prevention and intervention strategies can be designed. The model formulation process clarifies assumptions, variables, and parameters. Mathematical models provide results such as thresholds, basic reproduction numbers, contact numbers, and replacement numbers. These results can help health workers understand and predict the spread of an epidemic and evaluate the potential effectiveness of the different control measures to be used. They can improve the understanding of the relationship between social and biological factors that influence the spread of a diseases. Mathematical models and computer simulations are useful experimental tools for building and testing theories, answering specific questions and estimating key parameters from data.

The 2014 Ebola disease outbreak attracted many researchers with its rapid spread and high case fatality rate. It revealed the weaknesses and breaches of research on Ebola. Several mathematical models of EVD transmission dynamics have been formulated and studied to make projections and evaluate control strategies for disease eradication [25, 26, 27]. Most of these researchers looked at the effects of socio-economic factors such as the lack of sufficient hospital resources (hospital beds, medical caregivers, drugs and vaccines, laboratory equipment, quarantine facilities, emergency response services, information systems, and so on), human behaviour of the inhabitants of such communities, poverty, cultural and religious beliefs and practices of the people, burial of deceased individuals, on the transmission and control of EVD, (see [10, 9, 7, 12, 13, 14, 15, 16, 17]).

However, none of them studied the effects of war or any form of instability on the transmission and control of EVD. The presence of war or any form of instability can greatly interrupt or stop

the implementation of control strategies such as vaccination processes, construction and successful running of EVD treatment units (usually temporary tents in which infected individuals are isolated for treatment), proper functioning of intervention teams, which can intern increase the transmission and death rates. The recent WHO report on EVD in the Democratic Republic of Congo says, "Repeated bouts of violence have hampered the ability of the response teams to do their work and the virus has taken advantage of their limitation. Also, efforts to vaccinate people who have been in contact with infected persons have been suspended for the day because of the previous day's attack", see [17]

Our model, therefore, presents a study of EVD dynamics in the presence of interfered control where the main object of interference is war or political instability.

2. MODEL FORMULATION

EVD transmission is mostly either by person to person contacts or individuals coming in contact with objects that have come in contact with infected individuals. It is important to note that in the presence of war, the contact rate is assumed to be higher. The specific component of war we are interested in is the impact of war, measured by a parameter ω, defined as the level of impact of war on infection and hospitalization. With regards to hospitalization, the parameter ω measures the proportion of the infected population that is not being hospitalized as a result of the war. As the level of war increases, infection rate increases and hospitalization rate decreases. However, we assume that $0 < \omega < 1$ and the increase in the infection rate with respect to ω is non-linear and saturating. There is, therefore, a need to propose a contact rate function β that is dependent on the level of war. We propose the following contact function.

$$\beta(\omega) = \frac{\beta_{max}}{1 + Ae^{-K\omega}}. \tag{1}$$

The constant A is the scale parameter and K is the shape parameter. The parameter A is such that $1 << A < \infty$. Thus, if the level war is very high, the rate of spread of the disease through person to person contact will be approximately β_{max}. The parameter K determines how fast the impact of war can be felt. Note that if $\omega = 1$, $\beta(\omega) \to \beta_{max}$ as $K \to \infty$. Therefore, the parameter K must be chosen such that $\beta(\omega) \to \beta_{max}$ as $\omega \to 1$. A typical example of change in contact rate against the level of interference is shown in Fig 1. To evaluate the Ebola virus

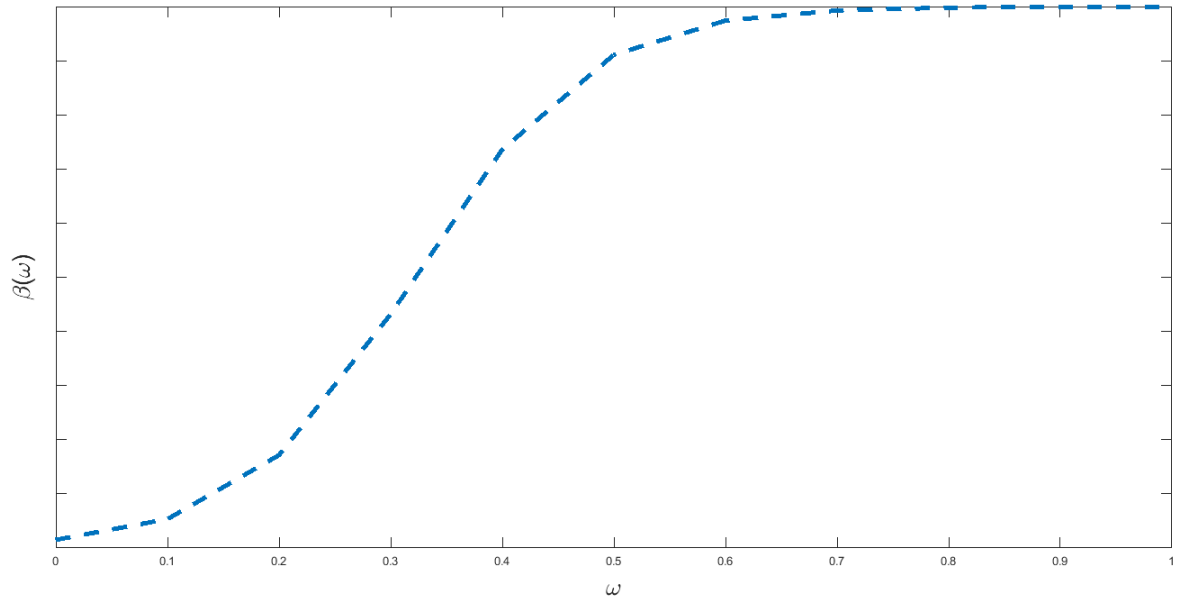

FIG. 1. Contact rate as a function of level of interference

disease dynamics in the presence of interrupted interventions or interfered control, where the main object of interference is war, we formulate a deterministic model of five compartments. The human population size $N(t)$ comprises of individuals that are susceptible $S(t)$, infected $I(t)$, hospitalized $H(t)$, recovered $R(t)$, or deceased $D(t)$. Thus the population at any time t is:

$$N(t) = S(t) + I(t) + H(t) + R(t) + D(t).$$

Individuals are recruited into the susceptible class at a rate proportional to the total population size $N(t)$. The size of the total population is assumed constant $N(t)$ because it has not varied considerably during the modelling time (in months). After exposure to the Ebola virus, susceptible individuals become infected and move to the infected compartment. The force of infection is given by:

$$\lambda(t) = \beta(\omega)\Big(I + \alpha_1 H + \alpha_2 D\Big) \tag{2}$$

where $\beta(\omega)$ is the effective transmission rate, that depends on the level of interference ω, α_1 and α_2 are relative infectivity rates. Hospitalized individuals are assumed to be infectious, but with lower infectivity than individuals in class I because of the controlled environment in which they are isolated. So, $0 < \alpha_1 < 1$. Since dead bodies of EVD deceased are highly infectious, we

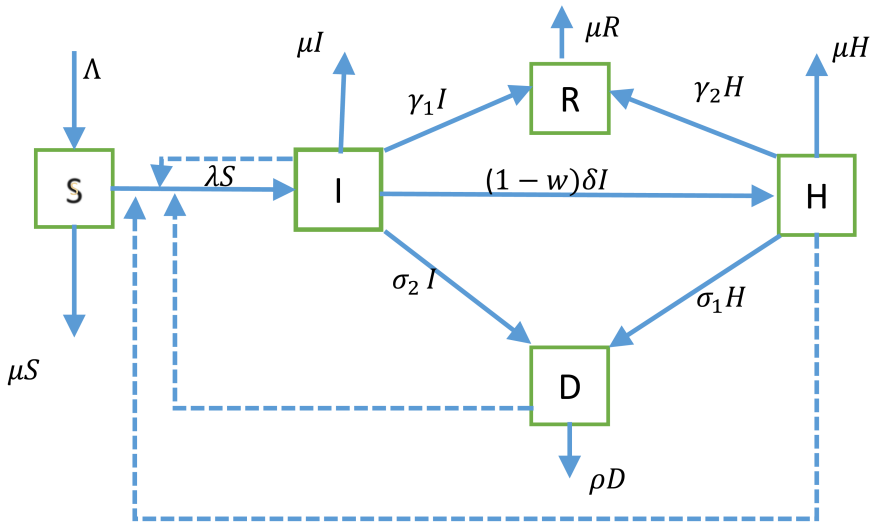

FIG. 2. Compartmental diagram showing population dynamics in the presence of interrupted interventions

assume that $\alpha_2 > 1$. When access to Ebola treatment units or hospitals is guaranteed, infected individuals can either be hospitalized at a per capita rate $(1-\omega)\delta$ or die from the disease at a rate σ_2, or in some rare cases recover at a rate γ_1. We assume that when $\omega = 1$, hospitalization becomes impossible, leading to an increase in disease transmission. However, no matter how low the level of interference gets, even in the complete absence of interference (war), at least there will be some level of contact, and hence infectivity will always be there.

Hospitalized EVD patients can recover at a rate γ_2 or die at a rate σ_1 because of the disease. The natural death rate μ is assumed for each class and dead bodies are disposed at a rate ρ. The flows between different compartments of the model are represented by Fig 2. The flow diagram and the model assumptions give rise to the following system of equations.

$$\frac{dS}{dt} = \Lambda - \lambda S - \mu S, \tag{3}$$

$$\frac{dI}{dt} = \lambda S - (\mu + \gamma_1 + \sigma_2 + (1-\omega)\delta)I, \tag{4}$$

$$\frac{dR}{dt} = \gamma_1 I - \mu R + \gamma_2 H, \tag{5}$$

$$\frac{dH}{dt} = (1-\omega)\delta I - (\mu + \gamma_2 + \sigma_1)H, \tag{6}$$

$$\frac{dD}{dt} = \sigma_1 H + \sigma_2 I - \rho D, \tag{7}$$

where $S(0) > 0$, $I(0) \geq 0$, $R(0) \geq 0$, $H(0) \geq 0$, $D(0) \geq 0$, $\forall\, t \geq 0$.

Since the recovered individuals do not contribute to disease transmission, the system can then be reduced to the following:

$$\frac{dS}{dt} = \Lambda - (\lambda + \mu)S, \tag{8}$$

$$\frac{dI}{dt} = \lambda S - \Big(Q_1 + (1-\omega)\delta\Big)I, \tag{9}$$

$$\frac{dH}{dt} = (1-\omega)\delta I - Q_2 H, \tag{10}$$

$$\frac{dD}{dt} = \sigma_1 H + \sigma_2 I - \rho D, \tag{11}$$

where $Q_1 = \mu + \gamma_1 + \sigma_2$, $Q_2 = \mu + \sigma_1 + \gamma_2$, and λ is as defined in equation (2)

3. Model Properties and Analysis

3.1. Positivity of solutions. We need to ensure that the variables remain non-negative and solutions of the system are non-negative $\forall\, t \geq 0$, given any non-negative initial conditions. We thus have the following theorem.

Theorem 1. *Given the initial conditions $S(0) > 0$, $I(0) \geq 0$, $H(0) \geq 0$, $D(0) \geq 0$, the solutions $S(t)$, $I(t)$, $H(t)$, $D(t)$ of the system (8)-(11) remain non-negative $\forall\, t \geq 0$.*

Proof. To show non-negativity of solutions, it is sufficient to show that each of the solutions of the system (8)-(11) is non-negative $\forall\, t \geq 0$.

From (8), the differential inequality describing the evolution of the susceptible population over time is given by:

$$\frac{dS}{dt} \geq -(\lambda(t) + \mu)S(t).$$

By separating variables in the differential inequality and solving using simple integration and Gronwall inequality, we have that:

$$S(t) \geq S(0)\exp\Big(-\Big(\int_0^t \lambda(\tau)d\tau + \mu t\Big)\Big) > 0.$$

Similarly, from (9),

$$\frac{dI}{dt} \geq -(Q_1 + (1-\omega)\delta)I(t).$$

Therefore,

$$I(t) \geq I(0)\exp\Big(Q_1 t + (1-\omega)\delta t\Big) \geq 0.$$

Similarly, from (10),

$$\frac{dH}{dt} \geq -Q_2 H(t),$$

so that,

$$H(t) \geq H(0)\exp\Big(-Q_2 t\Big) \geq 0.$$

Finally, from (11),

$$\frac{dD}{dt} \geq -\rho D,$$

and therefore,

$$D(t) \geq D(0)\exp\Big(-\rho t\Big) \geq 0.$$

Thus all the solutions of the system are non-negative for any non-negative initial conditions. □

3.2. Invariant region.

Theorem 2. *The system (8)-(11) is biologically meaningful in the region:*

$$\Omega = \left\{ \Big(S(t), I(t), H(t), D(t)\Big) \in \mathbb{R}^4 : m(t) \leq \frac{\Lambda}{\mu},\ D(t) \leq \frac{(\sigma_1+\sigma_2)}{\rho} \right\},$$

where the basic properties of existence, uniqueness and continuity of solution are valid for the Lipschitzian system (8)-(11), and

$$m(t) = S(t) + I(t) + H(t).$$

Proof.

Given that,

$$m(t) = S(t) + I(t) + H(t),$$

adding the equations (8)-(10) yields

$$\frac{dm}{dt} = \Lambda - \mu m. \tag{12}$$

From equation (12),

$$\frac{d}{dt}\Big(m\exp(\mu t)\Big) = \Lambda\exp(\mu t).$$

Integrating, we obtain:

$$m\exp(\mu t) - m_0 = \frac{\Lambda}{\mu}\exp(\mu t) - \frac{\Lambda}{\mu}$$

Thus,

$$m(t) = \frac{\Lambda}{\mu} + \Big(m_0 - \frac{\Lambda}{\mu}\Big)\exp(-\mu t) \tag{13}$$

For $m_0 > \dfrac{\Lambda}{\mu}$, we have $m(t)$ maximum at $t = o$. that is, $m(t) \leq m(o) = m_0 \; \forall \, t$.

For $m_0 < \dfrac{\Lambda}{\mu}$, we have $m_0 - \dfrac{\Lambda}{\mu} < 0$, and therefore $m(t)$ is maximum at $t = \infty$, that is, $m(t) \leq \dfrac{\Lambda}{\mu}$.

Hence,

$$m(t) \leq max\Big\{\frac{\Lambda}{\mu}, m_0\Big\}, \; \forall \, t \geq 0.$$

Therefore, $m(t)$ is bounded above $\forall \, t \geq 0$.

Similarly, $I(t) < m(t) < \dfrac{\Lambda}{\mu}$ and $H(t) < m(t) < \dfrac{\Lambda}{\mu}$.

Also, from equation (11), we have that

$$\frac{dD}{dt} \leq \Big(\sigma_1 + \sigma_2\Big) - \rho D. \tag{14}$$

Therefore,

$$\frac{d}{dt}\Big(D\exp(\rho t)\Big) = (\sigma_1 + \sigma_2)\exp(\rho t).$$

Integrating, we have,

$$D\exp(\rho t) - D_0 = \Big(\frac{\sigma_1 + \sigma_2}{\rho}\Big)\exp(\rho) - \Big(\frac{\sigma_1 + \sigma_2}{\rho}\Big).$$

Therefore,

$$D(t) = \Big(\frac{\sigma_1 + \sigma_2}{\rho}\Big) + \Big(D_0 - \Big(\frac{\sigma_1 + \sigma_2}{\rho}\Big)\Big)\exp(-\rho t).$$

For $D_0 > \Big(\dfrac{\sigma_1 + \sigma_2}{\rho}\Big)$, we have $D(t)$ maximum at $t = 0$. That is, $D(t) \leq D_0 \; \forall \, t$.

For $D_0 < \Big(\dfrac{\sigma_1 + \sigma_2}{\rho}\Big)$, we have $\Big(D_0 - \Big(\dfrac{\sigma_1 + \sigma_2}{\rho}\Big)\Big) < 0$, and therefore, $D(t)$ is maximum at

$t = \infty$. That is, $D(t) \leq \left(\frac{\sigma_1 + \sigma_2}{\rho}\right)$.

Hence,

$$D(t) =\leq max\left\{\left(\frac{\sigma_1 + \sigma_2}{\rho}\right), D_0\right\} \forall\, t \geq 0$$

Therefore, $D(t)$ is bounded above $\forall\, t$.

We can conclude that Ω is positively invariant and attracts all positive solutions of the system (8)-(11). □

3.3. Disease free equilibrium. The inclusion of demographic dynamics may permit the disease to persist in the population for a long time. One of the most useful ways of thinking about what may happen eventually is to explore when the system is at equilibrium. We obtain the disease-free equilibrium by setting the right-hand side of the system (8)-(11) to zero. In the absence of Ebola, $I^* = H^* = D^* = 0$. If we substitute these into (8), we have

$$S^* = \frac{\Lambda}{\mu}.$$

Therefore the disease free equilibrium point is given by:

$$E_0 = \left(S^*, I^*, H^*, D^*\right) = \left(\frac{\Lambda}{\mu}, 0, 0, 0\right).$$

Before we look at the disease endermic state, we first determine the model reproduction number and consider the stability of the disease free equilibrium which we shall call the Ebola-free equilibrium.

3.4. The effective reproduction number. In this model, new infections are generated either by person to person contact or by contact between persons and pathogen infested objects. Thus, the effective reproduction number in the presence of interference $R_0 = R_\omega$ is defined as the average number of new infections generated by an infected individual in a completely susceptible population, [1] or through contact with a pathogen infested object. R_ω often serves as a threshold parameter that predicts whether an infection will spread or not. We use the next-generation matrix method, see [5], to compute R_ω by transforming the system (8)-(11) into the following:

$$\begin{pmatrix} \frac{dI}{dt} \\ \\ \frac{dH}{dt} \\ \\ \frac{dD}{dt} \end{pmatrix} = \begin{pmatrix} \lambda S \\ \\ 0 \\ \\ 0 \end{pmatrix} - \begin{pmatrix} Q_1 I + (1-\omega)\delta I \\ \\ Q_2 H + (1-\omega)\delta I \\ \\ \rho D - \sigma_1 H - \sigma_2 I \end{pmatrix} = \mathscr{F} - \mathscr{V},$$

where $\mathscr{F}$ denotes the rate of occurrence of new infections and $\mathscr{V}$ denotes the rate of transfer of individuals into or out of each compartment [4]. The next-generation matrix is given by FV^{-1}, where F and V are the Jacobian matrices shown below, for some constant $\beta(\omega)$.

$$F = \begin{pmatrix} \frac{\pi}{\mu}\beta(\omega) & \frac{\pi}{\mu}\alpha_1\beta(\omega) & \frac{\pi}{\mu}\alpha_2\beta(\omega) \\ \\ 0 & 0 & 0 \\ \\ 0 & 0 & 0 \end{pmatrix} \quad V = \begin{pmatrix} Q_1 + (1-\omega)\delta & 0 & 0 \\ \\ (1-\omega)\delta & Q_2 & 0 \\ \\ -\sigma_2 & -\sigma_1 & \rho \end{pmatrix}.$$

The reproduction number $R_0 = R(\omega)$ is given as the spectral radius of matrix FV^{-1} which is classified as the next generation matrix. Therefore,

$$\begin{aligned} R_0 &= \rho\left(FV^{-1}\right) \\ &= \frac{\pi\beta(\omega)}{\mu\rho Q_2(Q_1 + (1-\omega)\delta)}\Big(\delta(1-\omega)(\rho\alpha_1 + \alpha_2\sigma_1) + Q_2(\rho + \alpha_2\sigma_2)\Big). \end{aligned}$$

Note that $R_0 = R_a + R_b + R_c$, where, $R_a = \dfrac{\pi\beta(\omega)}{\mu(Q_1 + (1-\omega)\delta)}$,

$$R_b = \frac{\pi\beta(\omega)\alpha_1(1-\omega)\delta}{\mu\Big(Q_1 + (1-\omega)\delta\Big)Q_2},\ R_c = \frac{\pi\beta(\omega)\alpha_2}{\mu\rho(Q_1 + (1-\omega)\delta)}\Big(\sigma_2 + \frac{\sigma_1(1-\omega)\delta)}{Q_2}\Big),$$

are the contributions of the infectious, hospitalized and dead individuals respectively to disease transmission.

4. Global Stability of the Disease Free Equilibrium

We have the following result on the global stability of E_0.

Theorem 3. *The disease free equilibrium E_0 of the model system (8)-(11) is globally asymptotically stable in the invariant region Ω whenever $R_\omega < 1$ and unstable otherwise.*

Proof. We choose a suitable Lyapunov function given by:

$$L(t) = I + v_1 H + v_2 D, \tag{15}$$

which involves individuals who directly contribute to the spread of the infection. The constants v_1, v_2, are all non-negative and we ought to find them. We note that the Lyapunov function, $L(t)$ is a C^1 and a positive definite function. The time derivative of the Lyapunov function $L(t)$ is given by:

$$\begin{aligned}
\frac{dL}{dt} &= \frac{dI}{dt} + v_1 \frac{dH}{dt} + v_2 \frac{dD}{dt}, \\
&= \lambda S - Q_1 I - (1-\omega)\delta I + v_1\Big((1-\omega)\delta I - Q_2 H\Big) + v_2\Big(\sigma_1 H - \rho D + \sigma_2 I\Big), \\
&= (\beta S - \psi + v_1(1-\omega)\delta + v_2\sigma_2)I + (\beta S\alpha_1 - Q_2 v_1 + v_2\sigma_1)H + \beta S\alpha_1 - \rho v_2)D,
\end{aligned}$$

where, $\psi = Q_1 + (1-\omega)\delta$. Note that at DFE, $S \leq \dfrac{\Lambda}{\mu}$. Therefore, the Lyapunov function L satisfies the inequality: [2ex]

$$\frac{dL}{dt} \leq \Big(\beta\frac{\Lambda}{\mu} - \psi + v_1(1-\omega)\delta + v_2\sigma_2\Big)I + \Big(\beta\frac{\Lambda}{\mu}\alpha_1 - Q_2 v_1 + v_2\sigma_1\Big)H + \Big(\beta\frac{\Lambda}{\mu}\alpha_1 - \rho v_2\Big)D. \tag{16}$$

We equate the coefficients of H and D to zero and solve for v_1 and v_2.

$$v_1 = \frac{\beta\Lambda(\rho\alpha_1 + \alpha_2\sigma_1)}{\mu\rho Q_2},\ v_2 = \frac{\Lambda\beta\alpha_2}{\mu\rho}.$$

Substituting the constants into the inequality 16 we obtain:

$$\frac{dL}{dt} \leq \psi(R_\omega - 1)I.$$

When $R_\omega \leq 1$, $\frac{dL}{dt}$ is negative semi-definite, with equality at $R_\omega = 1$ and, or $I \in E_0$. Therefore, the largest compact invariant set in Ω such that $\frac{dL}{dt} = 0$ is the singleton E_0. Therefore, by the LaSalle's Invariance Principle [19], the disease free equilibrium E_0 is globally asymptotically stable in Ω if $R_\omega \leq 1$ and unstable otherwise. □

Remark 1. *While we have defined the local stability of the disease free equilibrium, it is important to note that the global stability of the disease free equilibrium point implies its local stability.*

5. Existence and Stability of the Endemic Equilibrium

In this section we find the endemic equilibrium point of the system (8)-(11). Let the endemic equilibrium be represented by the phase space

$$E^{**} = \Big(S^{**}, I^{**}, H^{**}, D^{**}\Big) \in \mathbb{R}^4_+.$$

At the endemic equilibrium, each of the population phase space variables is constant, such that the rate of change of each of the components is zero. Thus,

$$\Lambda - (\lambda + \mu)S = 0, \tag{17}$$

$$\lambda S - \Big(Q_1 + (1-\omega)\delta\Big)I = 0, \tag{18}$$

$$(1-\omega)\delta I - Q_2 H = 0, \tag{19}$$

$$\sigma_1 H + \sigma_2 I - \rho D = 0. \tag{20}$$

We solve for each space variable in terms of I^{**} (in which Λ is as defined in equation 2) as follows:

From (17) and (18), we have that

$$S^{**} = \frac{\rho(\delta - \delta\omega)Q_2}{\beta(-\delta(-1+\omega))(\rho\alpha_1 + \alpha_2\sigma_1) + Q_2(\rho + \alpha_2\sigma_2)} = \frac{\Lambda}{\mu R_\omega},$$

and

$$I^{**} = \frac{\lambda}{\delta - \delta\omega + Q_1} - \frac{\mu\rho Q_2}{\beta(-\delta(-1+\omega))(\rho\alpha_1 + \alpha_2\sigma_1) + Q_2(\rho + \alpha_2\sigma_2)} = \frac{\Lambda}{\psi R_\omega}\Big(R_\omega - 1\Big).$$

From (19),

$$H^{**} = \frac{(1-\omega)\delta}{Q_2} I^{**},$$

and from (20),

$$D^{**} = \frac{Q_3}{Q_2 \rho} I^{**},$$

where $Q_3 = (\delta(1-\omega)\sigma_1 + Q_2\sigma_2)$.

Clearly, when $R_\omega > 1$, each of the state variables S^{**}, I^{**}, H^{**}, D^{**} is non-negative.

We thus have the following result on the existence of the endemic equilibrium point.

Theorem 4. *The model system (8)-(11) has a unique endemic equilibrium point* $E^{**} = \left(S^{**}, I^{**}, H^{**}, D^{**}\right)$ *that exists if and only if* $R_\omega > 1$.

Theorem 5. *The endemic equilibrium* E^{**} *is globally stable for* $R_\omega > 1$.

Proof. We set the Lyapunov function as:

$$\begin{aligned} V &= \left[S - S^{**} - S^{**} \ln\left(\frac{S}{S^{**}}\right)\right] + k_1\left[I - I^{**} - I^{**}\ln\left(\frac{I}{I^{**}}\right)\right] \\ &\quad + k_2\left[H - H^{**} - H^{**}\ln\left(\frac{H}{H^{**}}\right)\right] + k_3\left[D - D^{**} - D^{**}\ln\left(\frac{D}{D^{**}}\right)\right], \end{aligned}$$

where k_1, k_2, k_3 are positive constants to be determined. At endemic equilibrium, $V(E^{**}) = 0$. The partial derivatives with respect to each variable are:

$$\frac{\partial V}{\partial S} = \left(1 - \frac{S^{**}}{S}\right), \ \frac{\partial V}{\partial I} = \left(1 - \frac{I^{**}}{I}\right),$$

$$\frac{\partial V}{\partial H} = \left(1 - \frac{H^{**}}{H}\right), \ \frac{\partial V}{\partial D}\left(1 - \frac{D^{**}}{D}\right).$$

So the endemic state is a critical point of V and the second derivatives are:

$$\frac{\partial^2 V}{\partial S^2} = \frac{S^{**}}{S^2}, \quad \frac{\partial^2 V}{\partial I^2} = k_1 \frac{I^{**}}{I^2},$$

$$\frac{\partial^2 V}{\partial H^2} = k_2 \frac{H^{**}}{H^2}, \quad \frac{\partial^2 V}{\partial D^2} = k_3 \frac{D^{**}}{D^2}.$$

The second derivative being positive at any point in Ω, the Lyapunov function V is concave up and the endemic equilibrium point is a minimum point of V. We now prove that $\frac{dV}{dt} \leq 0$. The time derivative of V is given by:

$$\begin{aligned}
\frac{dV}{dt} &= \Big(1-\frac{S^{**}}{S}\Big)\frac{dS}{dt} + k_1\Big(1-\frac{I^{**}}{I}\Big)\frac{dI}{dt} + k_2\Big(1-\frac{H^{**}}{H}\Big)\frac{dH}{dt} + k_3\Big(1-\frac{D^{**}}{D}\Big)\frac{dD}{dt}, \\
&= \Big(1-\frac{S^{**}}{S}\Big)\Big(\Lambda - \beta SI - \beta S\alpha_1 H - \beta S\alpha_2 D - \mu S\Big) + k_1\Big(1-\frac{I^{**}}{I}\Big) \\
&\quad \Big(\beta SI + \beta S\alpha_1 H + \beta S\alpha_2 D - Q_1 I - (1-\omega)\delta I\Big) + k_2\Big(1-\frac{H^{**}}{H}\Big) \\
&\quad \Big((1-\omega)\delta I - Q_2 H\Big) + k_3\Big(1-\frac{D^{**}}{D}\Big)\Big(\sigma_1 H - \rho D + \sigma_2 I\Big).
\end{aligned} \tag{21}$$

At endemic equilibrium, the system (8)-(11) yields:

$$\begin{aligned}
\pi &= (\beta I^{**} + \beta\alpha_1 H^{**} + \beta\alpha_2 D^{**})S^{**},\ \rho = \frac{\sigma_1 H^{**} + \sigma_2 I^{**}}{D^{**}}, \\
Q_1 &= \frac{(\beta I^{**} + \beta\alpha_1 H^{**} + \beta\alpha_2 D^{**})S^{**} - (1-\omega)\delta I^{**}}{I^{**}},\ Q_2 = \frac{(1-\omega)\delta I^{**}}{H^{**}}.
\end{aligned} \tag{22}$$

Replacing expressions from the system (22) into equation (21) yields:

$$\begin{aligned}
\frac{dV}{dt} &= \Big(1-\frac{S^{**}}{S}\Big)\Big[\beta S^{**}I^{**}\Big(1-\frac{SI}{S^{**}I^{**}}\Big) + \alpha_1\beta S^{**}H^{**}\Big(1-\frac{SH}{S^{**}H^{**}}\Big) \\
&\quad + \alpha_2\beta S^{**}D^{**}\Big(1-\frac{SD}{S^{**}D^{**}}\Big) + \mu(S^{**}-S)\Big] + k_1\Big(1-\frac{I^{**}}{I}\Big)\Big[\beta S^{**}I^{**}\Big(\frac{SI}{S^{**}I^{**}} - \frac{I}{I^{**}}\Big) \\
&\quad + \alpha_2\beta S^{**}D^{**}\Big(\frac{SD}{S^{**}D^{**}} - \frac{I}{I^{**}}\Big)\Big] + k_2\Big(1-\frac{H^{**}}{H}\Big)\delta(1-\omega)I^{**}\Big(\frac{I}{I^{**}} - \frac{H}{H^{**}}\Big) \\
&\quad + k_3\Big(1-\frac{D^{**}}{D}\Big)\Big[\sigma_1 H^{**}\left(\frac{H}{H^{**} - \frac{D}{D^{**}}}\right) + \sigma_2 I^{**}\Big(\frac{I}{I^{**}} - \frac{D}{D^{**}}\Big)\Big].
\end{aligned} \tag{23}$$

Let

$$x = \frac{S}{S^{**}}, \qquad y = \frac{I}{I^{**}}, \qquad z = \frac{H}{H^{**}},$$

(24)

$$w = \frac{D}{D^{**}}, \quad H^{**} = g_1 I^{**}, \quad D^{**} = g^2 I^{**},$$

where,

$$g_1 = \frac{(1-\omega)\delta}{Q_2},\ g_2 = \frac{Q_3}{Q_2}.$$

Substituting the expressions in (24) into $\frac{dV}{dt}$, we have:

$$\frac{dV}{dt} = -\mu\frac{(S-S^{**})^2}{S} + \beta I^{**} f(x,y,z,w),$$

where,

$$\begin{aligned} f(x,y,z,w) &= \Big(1-\frac{1}{x}\Big)S^{**}\Big[(1-xy)+\alpha_1 g_1(1-xz)+\alpha_2 g_2(1-xw)\Big] \\ &\quad +k_1\Big(1-\frac{1}{y}\Big)S^{**}\Big[(xy-y)+\alpha_1 g_1(xz-y)+\alpha_2 g_2(xw-y)\Big] \\ &\quad +\frac{k_3}{\beta}\Big(1-\frac{1}{w}\Big)\Big[\sigma_1 g_1(z-w)+\sigma_2(y-w)\Big]\frac{k_2}{\beta}\delta(1-\omega)(y-z). \end{aligned}$$

Expanding and grouping coefficients of the same variable, we have:

$$\begin{aligned} f(x,y,z,w) &= \frac{k_2(1-\omega)\delta}{\beta} + \frac{k_3(g_1\sigma_1+\sigma_2)}{\beta} + S^{**}(k_1+1) + S^{**}(k_1+1)\alpha_1 g_1 \\ &\quad +S^{**}(K_1+1)\alpha_2 g_2 + y\Big(\frac{\delta(1-\omega)k_2}{\beta} + \frac{k_3\sigma_2}{\beta} \\ &\quad +S^{**}(1-k_1) - S^{**}g_1 k_1\alpha_1 - g_2 k_1\alpha_2 S^{**}\Big) + \frac{y}{z}\Big(-\frac{k_2(1-\omega)\delta}{\beta}\Big) \\ &\quad +z\Big(-\frac{k_2(1-\omega)\delta}{\beta} - \frac{g_1 k_3\sigma_1}{\beta} - g_1\alpha_1 S^{**}\Big) + w\Big(\frac{(g_1\sigma_1+\sigma_2)k_3}{\beta} - g_2\alpha_2 S^{**}\Big) \end{aligned}$$

$$+\frac{y}{w}\Big(-\frac{k_3\sigma_2}{\beta}\Big)+\frac{z}{w}\Big(-\frac{g_1k_3\sigma_1}{\beta}\Big)+xy(k-1)S^{**}+wx(g_2k_1\alpha_1-g_2\alpha_2)S^{**}$$

$$+\frac{wx}{y}(-g_2k_1\alpha_2S^{**})+\frac{xz}{y}(-g_1k_1\alpha_1S^{**})+xz(g_1k_1\alpha_1-g_1\alpha_1)S^{**}$$

$$+x(-k_1S^{**})+\frac{1}{x}\Big(-1-g_1\alpha_1-g_2\alpha_2\Big)S^{**}.$$

We now set the terms containing variables and with non-negative coefficients to zero in order to get rid of the positive and non constant part of f. The coefficients of y, z, u, xy and ux are thus set to zero and solved for k_1, k_2 and k_3. We obtain:

$$k_1=1,\ k_2=\frac{\beta}{1-\omega}\Big(\alpha_1g_1+\sigma_1g_1\frac{\alpha_2g_2}{\sigma_1g_1+\sigma_2}\Big)S^{**},\ k_3=\beta\frac{\alpha_2g_2}{\sigma_1g_1+\sigma_2}S^{**}.$$

Then,

$$\begin{aligned} f(x,y,z,w) &= \frac{k_2(1-\omega)\delta}{\beta}\Big(3-\frac{1}{x}-\frac{zx}{y}-\frac{y}{z}\Big)+\frac{k_3\sigma_2}{\beta}\Big(3-\frac{1}{x}-\frac{y}{w}-\frac{xw}{y}\Big) \\ &\quad +\frac{k_3\sigma_1g_1}{\beta}\Big(1+\frac{zx}{y}-\frac{xw}{y}-\frac{z}{w}\Big)+\Big(2-x-\frac{1}{x}\Big)S^{**}. \end{aligned} \tag{25}$$

We need to prove that $\dfrac{dV}{dt}\leq 0$. We already have the term $-\mu\dfrac{(S-S^{**})^2}{S}\leq 0$ from the expression of $\dfrac{dV}{dt}$. It is left for us to prove that $f(x,y,z,w)\leq 0$.

Applying the arithmetic mean geometric mean inequality stated in the Appendix, we have that

$$\frac{k_2(1-\omega)\delta}{\beta}\Big(3-\frac{1}{x}-\frac{zx}{y}-\frac{y}{z}\Big)\leq 0.$$

Similarly, we prove that the other terms of $f(x,y,z,w)$ in (25) are negative.

Then f is negative and will be equal to zero if $x=y=z=u=1$. So V is positive definite at the endemic equilibrium and $\dfrac{dV}{dt}\leq 0$ with equality in the set

$$G=\{(S,H,I,D):S=S^{**},I=I^{**},H=H^{**},D=D^{**}\}.$$

By LaSalle's invariance principle [11], E^{**} is globally asymptotically stable on Ω. □

6. NUMERICAL SIMULATIONS

In this section, we use Matlab to simulate the model. We first verify our theoretic conclusions related to stability analysis of the system (8)-(11), then we vary our parameter's values to better understand how interference influences the prevalence and transmission of EVD. This will be followed by data fitting in the model validation process. Hypothetically, we choose a population size of about 5.7 million people, which is approximately the size of the population of the North Kivu Province of the DRC. The initial conditions chosen are: $S_0 = 5,620000$, $I_0 = 80$, $H_0 = 0$, $D_0 = 0$.

6.1. Parameter estimation. There is a lot of uncertainty in the choice of parameter values for the model. This is because, some of the data from which parameters for models are chosen may be from experiments, case-control studies, clinical trials or surveys among others. All these methods are not completely error-proof even though efforts may be made to minimise possible errors. It is therefore important to carefully study the disease dynamics, put into consideration individual differences, location, social and economic contexts, while selecting the correct parameter values. In this section, therefore, we estimate some of the values of the parameters from existing literature to parameterize the model and the remaining parameters are estimated.
Since the mean infectious period for EVD is set to be from 4 to 10 days, the highest recovery rate γ_2 is set to $1/4$. Table 1 gives more details on the parameter values.

6.2. Sensitivity analysis. Sensitivity analysis is the process of ascertaining the degree to which an input parameter value affects the output of a model. The model system (8)-(11) has many parameters whose nominal values or parameter ranges are carefully estimated from published work. Since many of these parameters were not determined experimentally, their accuracy is not guaranteed. In the same way, the chosen parameter values are not chosen with absolute certainty but with some reasonable estimation. It is, therefore, necessary to establish the observed responses and influence of such parameters on the model. The establishment of such responses can be achieved through uncertainty or sensitivity analysis of the model parameters to the disease dynamics in case of an outbreak

TABLE 1. Model (8)-(11) parameter values.

Parameter	Description	Range	Source
π	Recruitment rate	120 day^{-1}	Estimated
β	Contact rate	$[10^{-7}, 0.1]$ day^{-1}	Estimated
μ	Natural death rate	0.0035	Estimated
σ_1	Disease related death of the infected	[0.005,0.9]day^{-1}	[3]
σ_2	Disease related death of the hospitalized	$[10^{-4} - 0.5]$ day^{-1}	Estimated
γ_1	Rate of recovery of the infected	[0.1,0.25] day^{-1}	[18]
γ_2	Rate of recovery of the hospitalized	0.25	Estimated
λ	Probability for a contact to be infectious	[0.2,1] day^{-1}	[24]
ρ	Rate of disposal of dead bodies	[0.05,0.5]	Estimated
δ	Rate of hospitalization of the infectious	[0.005, 0.4]	Estimated
ω	Level of war	[0,1]	Estimated

In our model's sensitivity analysis, we use the LHS (Latin hypercube sampling scheme) implemented in Matlab to ascertain the major contributors to the model output in relation to the parameters in the model. Since we need a baseline or predictor of whether the disease may break out or not if new infectious individuals get into the vulnerable population, we capitalize on the model's basic reproduction number. In this work, we consider all the parameters to be uncertain. We hypothetically provide the range in which the parameters' values fall. The simulations are run 1000 times to have a large sample size which will make the results more precise. We then evaluate the partial rank correlation coefficients (PRCCs) of the parameters of interest. The results of the simulations are given in the Tornado plot, Fig 3.

From Fig 3, the most sensitive parameters with a positive correlation to the reproduction number are Λ, β, ω, α_2 and σ_2. β is the effective transmission rate, which by definition drives the infection in the total population. ω contributes to decrease the number of hospitalised individuals while σ_1 and σ_2 contribute to increase the number of infectious deceased, who are α_2 times more infectious than the infected that are alive. Increasing these parameters with a

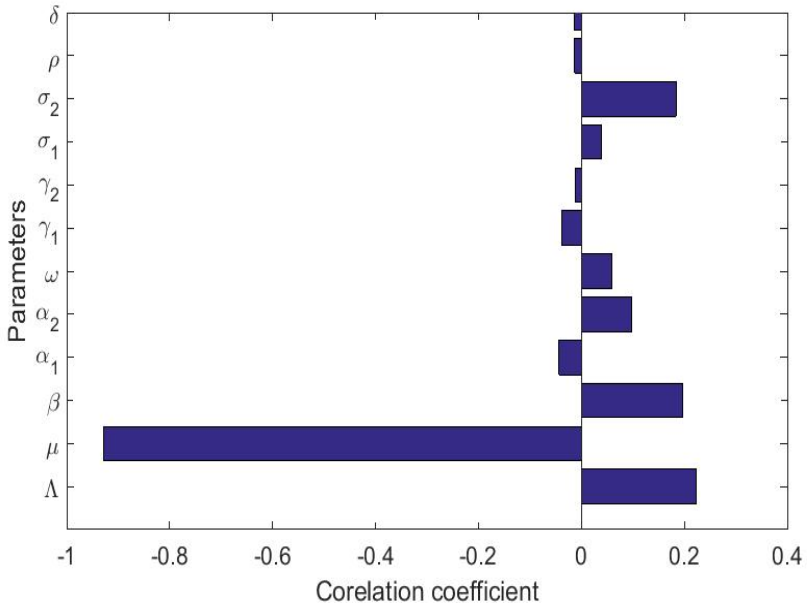

FIG. 3. Tornado plot showing some important parameters driving the EVD epidemic.

positive corelation coefficient will lead to an increase in the effective reproduction number R_ω, and hence an increase in the disease spread and transmission.

The parameter ρ has a negative correlation with R_ω since burials limit EVD transmission. Also, γ_1 and γ_2 have a negative correlation to R_ω. In fact, recovered individuals are assumed not to transmit EVD, hence, increasing these parameters will lead to a decrease in R_ω, and hence a decrease in disease transmission.

Fig 4 shows the Scatter plots of parameters with the more negative PRCCs. For these parameters, their increase results in a decrease in the epidemic.

7. SIMULATION RESULTS

Fig 5 shows how R_ω varies with the level of interference. The figure shows that the model reproduction number R_ω increases with war. We can actually use the graph to determine the value of R_ω for a given level of interference. We give an example that when $\omega = 0.8, R_\omega = 3.65$. This is actually important if we want to determine the level of war given a value of R_ω and vise versa.

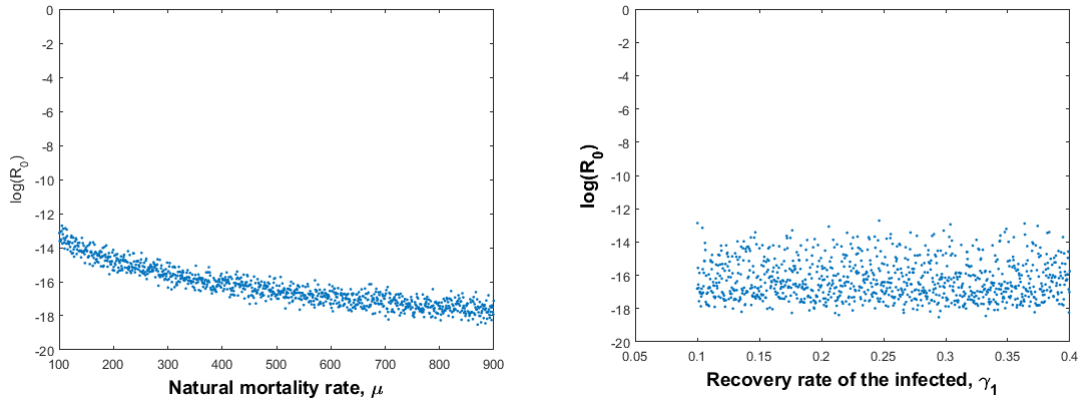

(a) (b)

FIG. 4. Scatter plots of parameters with the more negative PRCCs

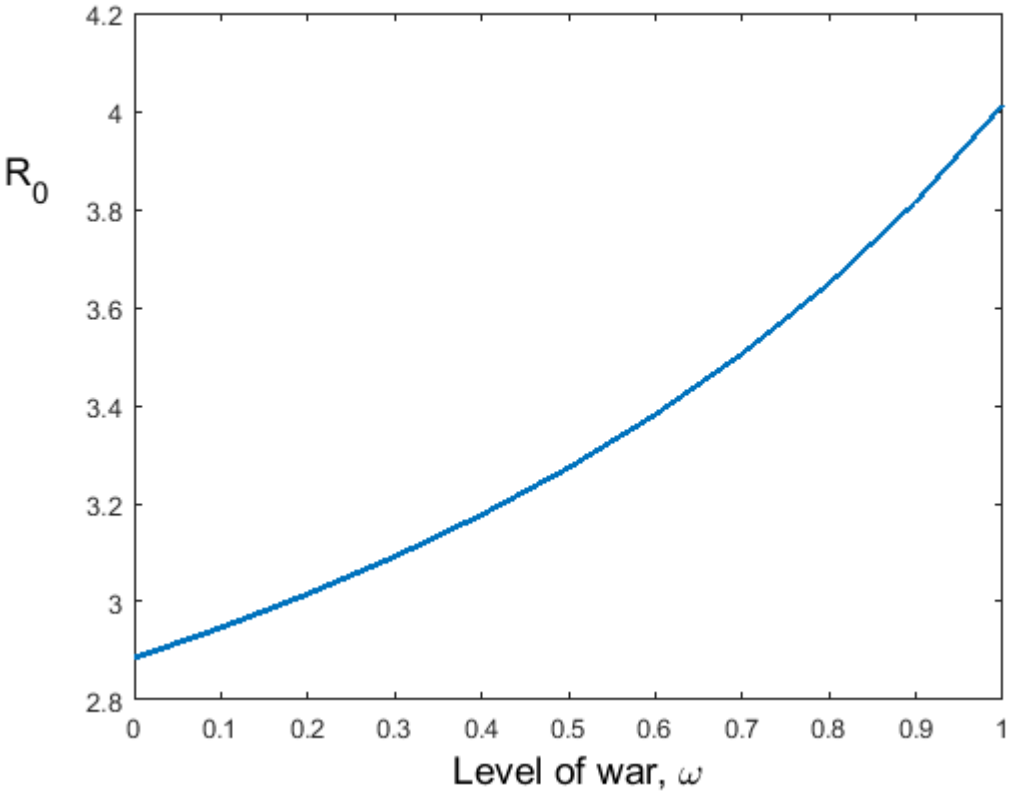

FIG. 5. R_ω as a function of level of interference (ω). The rest of the parameter values used are: $\Lambda = 120$, $\beta = 10^{-6}$, $\mu = 0.0035$, $\sigma_1 = 0.007$, $\sigma_2 = 0.005$, $\gamma_1 = 3 \times 10^{-4}$, $\gamma_2 = 8 \times 10^{-4}$, $\rho = 0.2$, $\delta = 8 \times 10^{-3}$, $\alpha_1 = 0.5$, $\alpha_2 = 1.2$. For these values, $R_\omega = 3.65$ when $\omega \approx 0.8$.

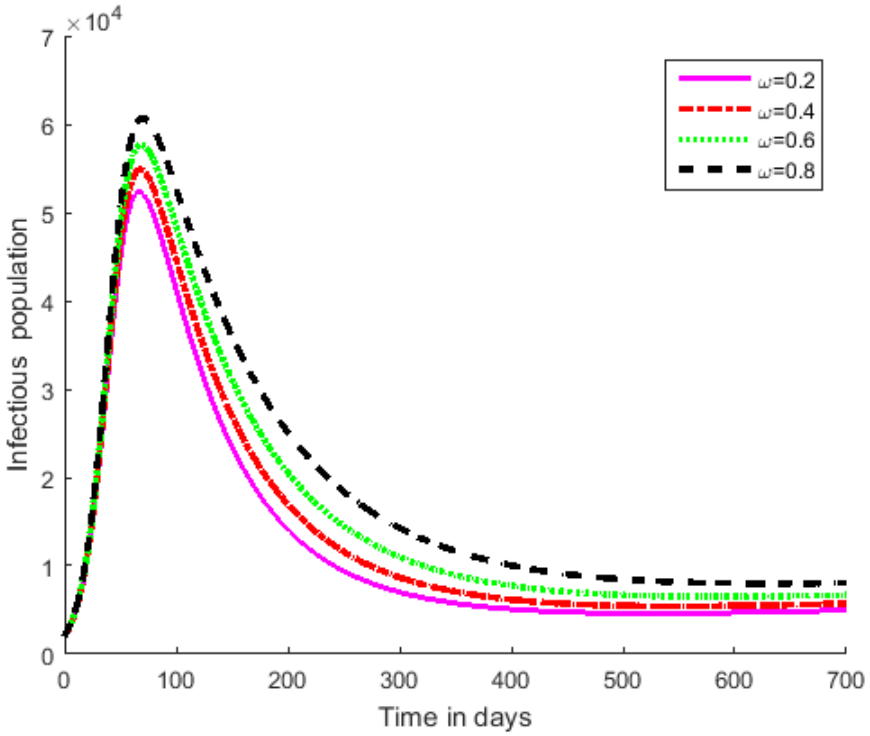

FIG. 6. Evolution of the infected population , for different levels of interference ω. The rest of the parameter values used are: $\Pi = 120$, $\beta = 10^{-6}$, $\mu = 0.0035$, $\sigma_1 = 0.007$, $\sigma_2 = 0.005$, $\gamma_1 = 3 \times 10^{-4}$, $\gamma_2 = 8 \times 10^{-4}$, $\rho = 0.2$, $\delta = 8 \times 10^{-3}$, $\alpha_1 = 0.5$, $\alpha_2 = 1.2$. For these values $R_\omega = 3.65$ when $\omega \approx 0.8$.

Figs 6 and 7 depict the effects of decreasing the level of interference on the number of infected and hospitalized individuals. We observe a slight decrease in the number of hospitalized cases and a slight increase in the number of infected individuals when the level of war is increased, indicating that, war alone does not induce a substantial change in the disease transmission process. The change is more noticeable with the hospitalized population. This may be because war interrupts hospitalization processes like construction and running of ETU's which are usually temporary tents, vaccination processes and also hinders the proper functioning of the intervention teams. The increase in the infected population as the level of interference increases shows that interference leads to an increase in the contact rate β. This is because interference interrupts hospitalization, thus, infected individuals can no longer be isolated in ETU's for treatment. This then leads to an increase in the person to person contact between susceptible individuals and infected individuals thus increasing disease transmission. Therefore preventing any form

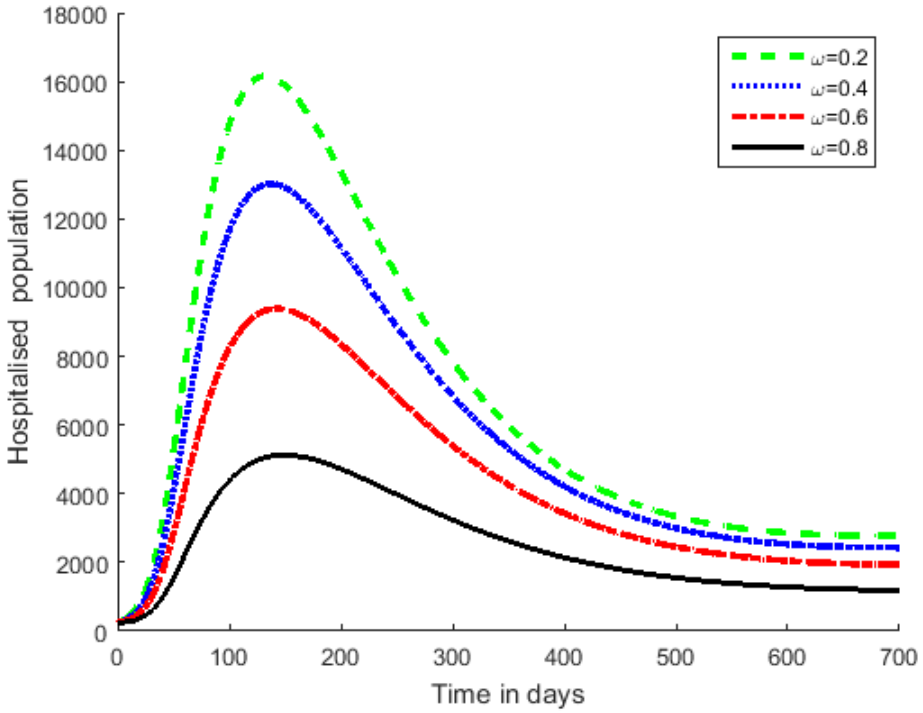

FIG. 7. Evolution of the population of the hospitalized, for different levels of interference ω. The rest of the parameter values used are: $\Pi = 120$, $\beta = 10^{-6}$, $\mu = 0.0035$, $\sigma_1 = 0.007$, $\sigma_2 = 0.005$, $\gamma_1 = 3 \times 10^{-4}$, $\gamma_2 = 8 \times 10^{-4}$, $\rho = 0.2$, $\delta = 8 \times 10^{-3}$, $\alpha_1 = 0.5$, $\alpha_2 = 1.2$. For these values $R_\omega = 3.65$ when $\omega \approx 0.8$.

of interference is important in containing the EVD outbreak. The reproduction number is made of parameters which differently influence its values. The relationship between those parameters can be evaluated through contour plots. We choose two parameters γ_1 and σ_2, and give the contour plots of R_ω as a function of ω and γ_1, and R_ω as a function of ω and σ_2. The contour plots in Fig 8 show that, when the level of war is very high (in an epidemic outbreak), the person-to-person contact rate increases and access to hospitalization facilities decrease. This leads to a decrease in the recovery rate and maximises disease transmission through contact with infected individuals. As such, the reproduction number R_ω increases and the disease related death rate also increases. The arbitrary values of R_ω on the R_ω-axis in Figures 8(a) and 8(b) indicate the corresponding relationship between the level of war and the recovery rate or the death rate of infected individuals respectively. At high values of R_ω, the outbreak may devastate the affected community and at low values of R_ω, the outbreak can be contained.

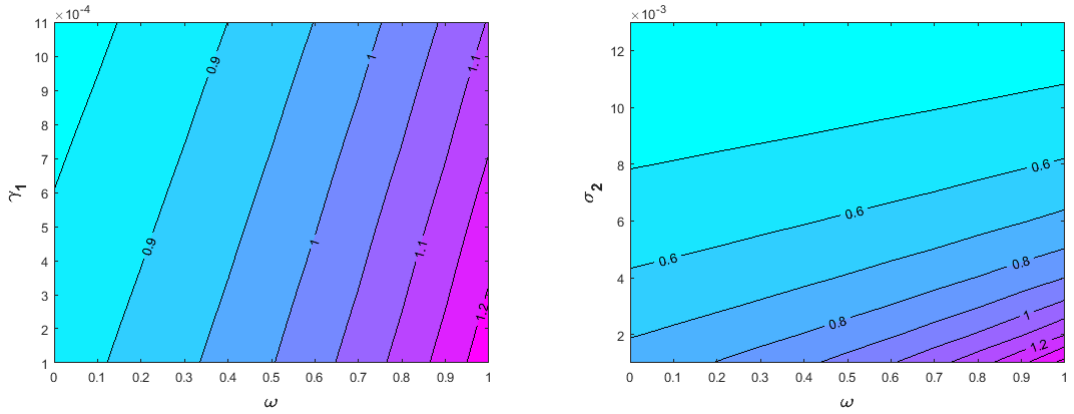

(a) (b)

FIG. 8. Contour plot of R_ω as a function of level of interference, ω and rate of recovery of the infected individuals, γ_1 and R_ω as a function of level of interference, ω and death rate of the infected individuals, σ_2.

8. MODEL VALIDATION

To validate our model, we use the WHO data obtained for the recent EVD epidemic in the Democratic Republic of Congo (DRC). We use data from the 2017-2019 outbreaks in the Kivu province in DRC as shown in table 2. The model presented in the system (8)-(11) is fitted to data in Table 2. The fitting process involves the use of the least square method in which, the unknown parameter values are given a lower bound and an upper bound from which the set of parameter values that produce the best fit are obtained. Fig 9 shows the fit of the model to the EVD data in Table 2. The model fits reasonably well to the data. The parameters that give the best fit are given in the caption. The reproduction number in this case is $R_\omega = 2.49$.

TABLE 2. Data from the 2018-2019 outbreaks in the Kivu province in DRC.

Date	Number of cases
05/08/2018	43
20/08/2018	102
02/09/2018	122
16/09/2018	142
02/10/2018	162
21/10/2018	238
11/11/2018	333
26/11/2018	421
10/12/2018	500
25/12/2018	585
14/01/2019	658
28/01/2019	743
10/02/2019	816
24/02/2019	872
10/03/2019	923
10/03/2019	1016
14/04/2019	1264
28/04/2019	1466
12/05/2019	1705
26/05/2019	1920
16/06/2019	2168
30/06/2019	2343
13/07/2019	2418
27/07/2019	2430

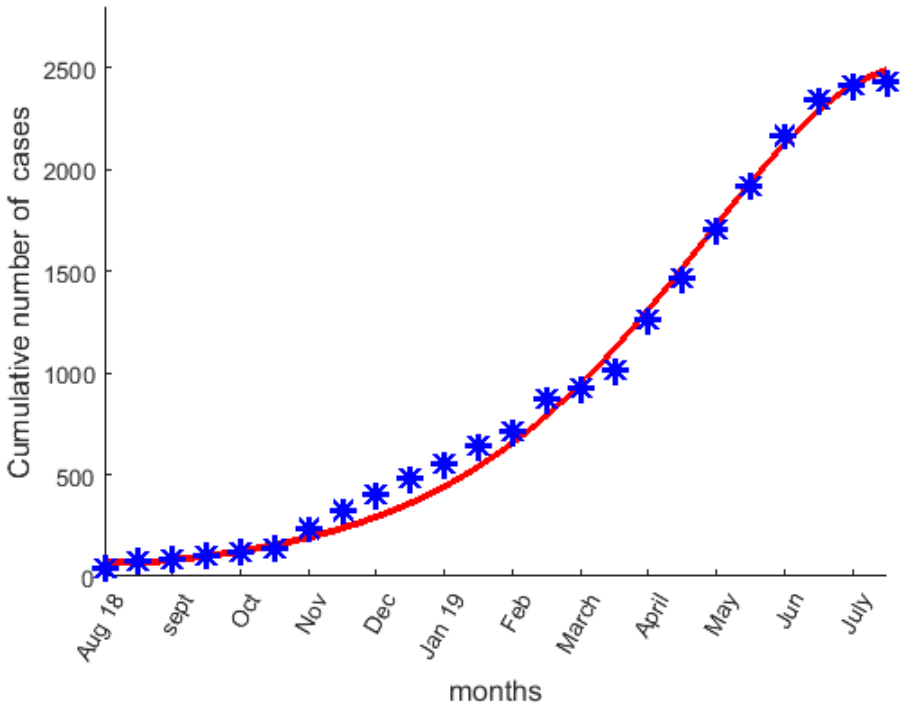

FIG. 9. Curve fitting for data from DRC. 18 and 19 on the x-axis stand for the years 2018 and 2019 respectively.

Fig 10 shows the effect of hospitalization on the infected population in the complete absence of war ($\omega = 0$). Note that, the absence of war or interference may not bring the population to a disease-free state as there exist other social and economic factors like poverty, religious beliefs and practices of the people, insufficient hospitalization facilities (hospital beds, medical caregivers, drugs and vaccines etc.), lack of media campaign etc, that lead to increase in the transmission and spread of the disease. However, in the absence of war or interference ($\omega = 0$), increasing hospitalization leads to a more rapid fall in the infection rate as shown in Fig 10.

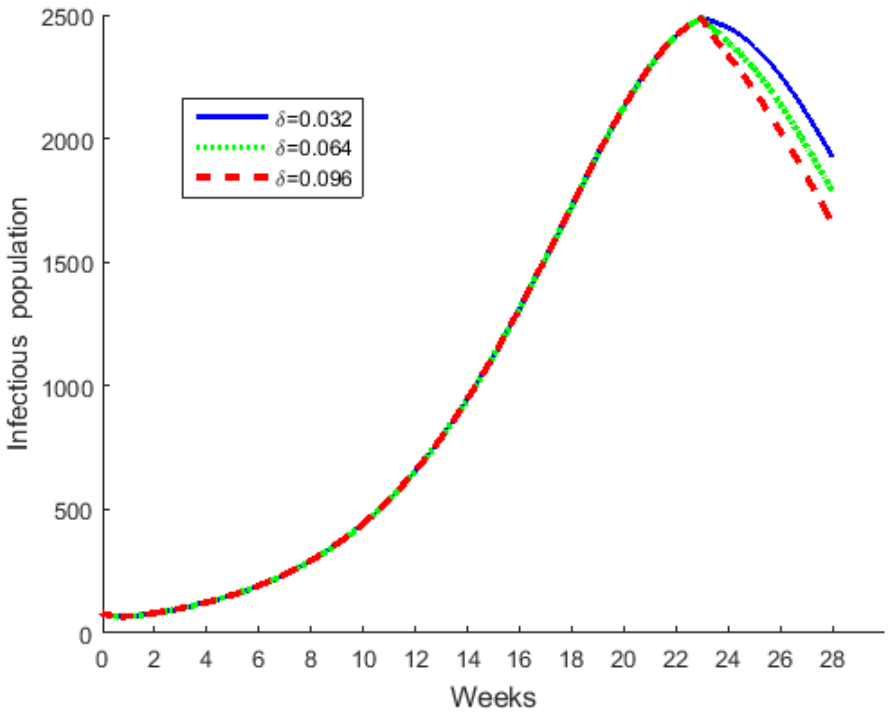

FIG. 10. Graph of delta variations in the complete absence of interference ($\omega = 0$). Note that the horizontal axis is now calibrated in weeks

9. CONCLUSION

In this chapter, a simple deterministic model that incorporates a war dependent person to person contact rate is presented and analyzed. Important mathematical features of the model such as the threshold for the epidemic, steady states, positivity and boundedness of solutions as well as the region of biological significance were determined. The model was shown to have a disease-free equilibrium which is globally asymptotically stable when the reproduction number is less than unity. This disease-free equilibrium is unstable when the disease threshold is greater than unity. The model also has an endemic equilibrium point that is globally stable whenever $R_\omega > 1$. Sensitivity analysis of the model parameters was carried out using the basic reproduction number as the threshold value with sampling based on the Latin Hypercube Sampling scheme. The output of the results of sensitivity analysis are indicated in the Tornado plot as well as the Scatter plots. The Tornado plot indicates the relative sensitivity of the parameters based on the obtained values of partial rank correlation coefficients. From the Tornado plot, the level

of interference has a positive PRCC of about 0.16. Therefore preventing interference would help contain the epidemic. We have also proven that the presence of interference to Ebola control efforts in a community undergoing an EVD epidemic is a determining factor in the disease control. It has been shown that when there is interference, controlling EVD is more difficult because interference makes hospitalization difficult and sometimes impossible.

As part of the model validation, the model was fitted to data from the Democratic Republic of Congo (DRC). The model formulated in this work is consistent with the dynamics of EVD in the DRC but is not without shortcomings. The lack of sufficient data on the number of Ebola cases recorded each month of the outbreak in the provinces affected by war limited the numerical analysis and interpretation. Other aspects like personal protective equipment and materials for laboratories have been useful in Ebola patients' management and care. These tools could also be taken into account. It is well documented that the goodness of fit measures the discrepancy between observed data and values expected from the model. In this work, no goodness of fit tests are done but we relied on the least-squares method for the model fitting. We, however, argue that the least-squares method of fitting models to data, provides useful insights into how the model can be linked to data despite the challenge of using statistical tools to test the goodness of fit of the model.

CONFLICT OF INTERESTS

The author(s) declare that there is no conflict of interests.

The authors (Maureen Juga and Farai Nyabadza) certify that they have no affiliations with or involvement in any organization or entity with any financial interest (such as honoraria; educational grants; participation in speakers' bureaus; membership, employment, consultancies, stock ownership, or other equity interest; and expert testimony or patent-licensing arrangements), or non-financial interest (such as personal or professional relationships, affiliations, knowledge or beliefs) in the subject matter or materials discussed in this manuscript.

REFERENCES

[1] Z. Mukandavire et al. Modelling and analysis of the intrinsic dynamics of cholera, Differ. Equ. Dyn. Syst. 19 (2011), 253–265.

[2] J.J. Muyembe et al. Ebola virus outbreaks in Africa: past and present, Onderstepoort J. Vet. Res. 79 (2012), 451.

[3] World Health Organisation, Ebola and Marburg virus disease epidemics: preparedness, alert, control and evaluation, WHO/HSE/PED/CED/2014.05, 2014.

[4] J. Diamond, STELLA Modelling of a Zombie Invasion, https://www.scribd.com/document/24096872/STELLA-Modeling-of-a-Zombie-Invasion, 2009.

[5] van Den Driessche P. et al. Reproduction numbers and sub-threshold endemic equilibria for compartmental models of disease transmission. Math. Biosci. 180 (2002), 29-48.

[6] Feldmann et al H, Ebola hemorrhagic fever, Lancet, 387 (2011), 849-862.

[7] S.D. Djiomba Njankou et al. Modelling the potential impact of limited hospital beds on Ebola virus disease dynamics, Math. Methods Appl. Sci. 41 (18) (2018), 8528-8544.

[8] World Health Organisation, Case definition recommendations for Ebola or Marburg virus diseases, http://www.afro.who.int (accessed in December 2014), 2014.

[9] A. Rachah, D.F.M. Torres, Mathematical modelling, simulation and optimal control of the 2014 Ebola outbreak in West Africa, Discr. Dyn. Nat. Soc. 2015 (2015), 842792.

[10] J.A. Lewnard et al. Dynamics and control of Ebola virus transmission in Montserrado, Liberia: A mathematical modelling analysis. Lancet Infect. Dis. 14 (2014), 1189-1195.

[11] J.P. LaSalle and Z. Artstein, The stability of dynamical systems, appendix A, limiting equations and stability of non-autonomous ordinary differential equations, Soc. Ind. Appl. Math. 15, 1876.

[12] E. Bonyah et al, An optimal control application to an Ebola model, Asian Pac. J. Trop. Biomed. 4 (2016), 283-286.

[13] W.H. McNeill, Plagues and people, Garden City, Anchor Press, 1976.

[14] S. Funk et al, Modelling the influence of human behaviour on the spread of infectious diseases: a review, J. R. Soc. Interface, 5 (2010), 1247-1256.

[15] S. Funk et al. Nine challenges in incorporating the dynamics of behaviour in infectious diseases models, Epidemics, 10 (2015), 21-25.

[16] M. Salathé and M. Bonhoeffer, The effect of opinion clustering on disease dynamics. Journal of the Royal Society, 5 (2008), 1505-1508.

[17] World Health Organisation, Ebola Response, annexes: key considerations for implementing a community care center (CCC), https://apps.who.int/iris/, 2014.

[18] J. Astacio et al. Mathematical models to study the outbreaks of Ebola. https://dspace.library.cornell.edu/bitstream/1813/31962/1/ BU-1365-M.pdf (accessed in December 2014), 2014.

[19] J.P. LaSalle, The stability of dynamical systems, Society for Industrial and Applied Mathematics, Philadelphia, 1976.

[20] H. Guo and M.Y. Li, Global stability of tuberculosis model with immigration and treatment, Can. Appl. Math. Q. 14 (2006), 185-198.

[21] F. Nyabadza et al. Modelling the HIV/AIDS epidemic trends in South Africa: insights from a simple mathematical model, Nonlinear Anal., Real Word Appl. 12 (2011), 2091-2104.

[22] C. Conell Mcclusky, Lyapunov functions for tuberculosis models with fast and slow progression, Math. Biosci. Eng. 3 (2006), 603-614.

[23] E. Bereta and V. Capasso, On general structure of epidemic systems: global asymptotical stability. Comput. Math. Appl. 12 (1989), 677-694.

[24] S.E. Bellan et al. Ebola control: effect of asymptomatic infection and acquired immunity. The Lancet, 384 (9953) (2014), 1499-1500.

[25] M.I. Meltzer et al. Estimating the future number of cases in the Ebola epidemic - Liberia and Sierra Leone, 2014-2015, Morbidity and Mortality Weekly Report, 63(03)(2014), 1-14.

[26] Feldmann H. and Geisbert T.W. Ebola hemorrhagic fever. Lancet, 387 (2011), 849-862.

[27] C.N. Haas, On the Quarantine Period for Ebola Virus. PLOS Currents Outbreaks, Edition 1. doi: 10.1371/currents.outbreaks.2ab4b76ba7263ff0f084766e43abbd89. 2014.

[28] New York Times, A Cure for Ebola? Two New Treatments Prove Highly Effective in Congo, https://www.nytimes.com/2019/08/12/health/ebola-outbreak-cure.html, 2019.

[29] Healthline, What to Know About a Potential Ebola 'Cure', https://www.healthline.com/health-news/what-to-know-about-a-potential-ebola-cure#Promising-breakthrough-against-Ebola, 2019.